Konrad-Zuse-Zentrum für Informationstechnik Berlin
Heilbronner Str. 10, D-10711 Berlin-Wilmersdorf

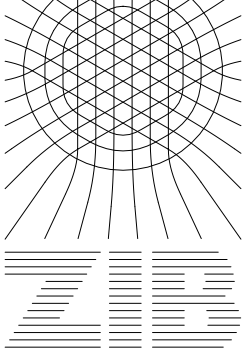

Rudolf Beck Peter Deuflhard Hans-Christian Hege
Martin Seebaß Detlef Stalling

Numerical Algorithms and Visualization in Medical Treatment Planning

Preprint SC-96-54 (December 1996)

Numerical Algorithms and Visualization in Medical Treatment Planning

Rudolf Beck Peter Deuflhard Hans-Christian Hege
Martin Seebaß Detlev Stalling

Abstract

After a short summary on therapy planning and the underlying technologies we discuss quantitative medicine by giving a short overview on medical image data, summarizing some applications of computer based treatment planning, and outlining requirements on medical planning systems. Then we continue with a description of our medical planning system HyperPlan. It supports typical working steps in therapy planning, like data aquisition, segmentation, grid generation, numerical simulation and optimization, accompanying these with powerful visualization and interaction techniques.

Preprint SC-96-54 (December 1996)

Contents

1 Introduction

New techniques for envisioning mathematical entities and advanced computer graphical algorithms have a positive effect on many application fields. One of the fastest growing areas with fastidious visualization applications is medicine. Two paradigm changes are currently taking place in medicine: diagnosis and therapy are increasingly based on the understanding of biochemical processes that cause the diseases, and, second, diagnosis and therapy are becoming more and more quantitative. The use of visualization techniques in medicine is mainly related to the second of these developments, the emergence of *quantitative medicine*. It allows a physician to taylor treatments individually, in general by utilizing a computer-based planning system. The enabling key technologies for computer-based treatment planning are 3D medical imaging methods.

Quantitative analyses of real phenomena require mathematical models that formally describe the relevant aspects. These descriptions have to be transformed into suitable algorithms to simulate the phenomena. In medical applications, however, the empirical input data are often incomplete, informations are difficult to valuate, and decisions are hard to formalize. Therefore only parts of medical problem domains can be formulated mathematically and in most medical planning tasks certain solution steps remain that cannot be automated. From an abstract point of view, these are the reasons why human beings remain an essential part of the problem solving process, even if advanced information processing techniques are at their disposal. Especially in critical medical cases both physicians and patients do not want to rely on automatic systems. Medical simulations therefore have to be controlled and monitored by a well trained medical staff, being able to supply additional information. The vast amount and high complexity of the data to be mediated to the medical expert make sophisticated *visualization techniques* indispensable. To be useful in a clinical environment medical planning software should also offer well designed user interfaces and advanced interaction techniques.

Software systems aiming at solving problems in quantitative medicine therefore require a synergetic combination of powerful interaction techniques, well chosen visualization methods and efficient algorithms from rather diverse fields like image processing, computational geometry, numerical mathematics and computer graphics.

In this paper we will present a framework, called HyperPlan, that supports the typical steps in 3D medical treatment planning. It provides basic functionality and can be extended easily for specific applications. To exemplify some of the system's features we concentrate on the application domain it

has originally been developed for: regional hyperthermia treatment planning. The system, however, is more general. Currently we are expanding it among other things for use in radiotherapy treatment planning and in gynecological applications.

The organisation of the paper is as follows. We start with a discusssion of quantitative medicine. After providing a short overview on medical image data, we summarize some applications where computer based treatment planning is already utilized. Based on these examples typical requirements on medical planning systems are outlined. Then the medical planning system HyperPlan is described: starting with the software design and a system overview, segmentation issues, grid generation, and numerical simulations are discussed. All steps in planning have to be accompanied by suitable visualization and interaction methods. Some of the techniques available in HyperPlan are discussed in the two following sections. We conclude with some remarks on the impact of scientific visualization on medical imaging and planning.

2 Computer Based Therapy Planning

2.1 Quantitative Medicine

Why using computers in medical diagnosis, treatment planning, and even treatments ? Human medical doctors are highly experienced in sensing visual, tactile, and other cues, as well as to pick up verbal and non-verbal expressions. They are able to grasp a comprehensive, holistic impression of the patient. Furthermore they can utilize a lot of largely unformalized knowledge on diagnostics and therapeutic procedures. And they are capable to improve with practice.

Computers, endowed with complementary capabilities, can support physicians in various tasks: For *diagnosis* they can perform the vast number of calculations necessary for 2D and 3D reconstruction, based on data from x-ray, nuclear magnetic resonance, or ultrasound tomography. These image data provide quantitative, patient-specific information that can be used in computer-aided *treatment planning*. For instance in cancer therapy data such as size, shape, position, and type of a tumor, as well as its position relative to adjacent (risk) organs can be considered. In order to individually plan a therapy or surgery, a mechanical, physiological, radiotherapeutical, thermal, endocrinological, or other model has to be simulated. On base of such simulations optimizations in parameter spaces can be performed, resulting in better treatment procedures. In order to guarantee a precise execution of the plans

developed, it is often necessary to accurately monitor and control instruments also *during* therapy and surgery. Furthermore a quantitative quality control is required to improve medical treatment procedures and simulation models.

On the whole, use of computers in medicine can help to significantly improve the efficacy of established therapeutical procedures and to make new methods of treatment possible. In the following we will concentrate on the planning aspects of quantitative medicine, starting with its basis, the medical image data.

2.2 3D Medical Imaging

The basis of medical planning are anatomical and functional data about the patient. With the advent of x-ray based computer tomography and, later, magnetic resonance imaging, a new discipline arose, 3D medical imaging. It employs techniques of computer vision, sometimes supplemented by methods of discrete and numerical mathematics, to extract from digital images the information useful for a given task. Furthermore, it utilizes visualization methods to display 3D structural information. 3D medical imaging therefore encompasses visualization, manipulation, and analysis of structure information captured in three- and higher-dimensional digital images [35, 32]. It has revolutionized diagnosis, therapy planning and many kinds of therapy.

Different physical phenomena are exploited for recording 3D medical images. Images of different 'modalities' therefore contain to some extend complementary information. Computer tomography (CT), based on the varying absorption of x-rays in different types of tissue, clearly reveals bony structures. Magnetic resonance imaging (MRI) distinguishes many soft tissue types. 3D ultrasound scanning provides similar information, but usually with less accuracy. Digital subtraction angiography (DSA), where x-ray images are taken with and without radioopaque dye injected into the patient's vascular system, provide images of the vascular anatomy. Positron emission tomography (PET), high field MRI, magneto-encephalography (MEG), and other techniques supply functional data like information about metabolic activities. The advantages of different physical techniques can be combined by taking images of the interesting region with different methods (mulitmodal imaging).

From a mathematical viewpoint a digital 3D image is a set of discrete samples $b(x_i)$ with $x_i \in \mathbf{R}^3$. The values or "grey levels" b of the image describe some physical quantity, e.g. optical density of the tissue for x-rays in case of CT images. Typically, these values are not measured directly, but are obtained from a complex mathematical reconstruction process. For

example for CT images an inverse Radon transformation has to be performed to obtain $b(x_i)$ from a set of x-ray projections. In the simplest case the sample points x_i form a rectangular grid with equi-distant spacings. However, due to technical reasons (e.g. helical scan methods, distortions) the sample points typically are less regularly distributed in space.

For the generation of expressive visualizations and the execution of numerical simulations anatomical entities like bones, muscles, organs, and so on have to be identified in the image domain: the data volume has to be partitioned into subsets corresponding to different tissue classes. This is the problem of (medical) *image segmentation*. There is a striking difference between digital image data, representing unstructured local information, and the structured perceptual information humans become aware of when looking at images. Therefore, segmentation is a more difficult task than one might assume. Segmenting a digital image means finding its homogeneous regions and its boundaries. Several hundreds or even more than thousand algorithms have been proposed for edge detection or region growing. Although rather general models of image segmentation exist, see e.g. [23], no algorithm works for a broad variety of applications. In clinical applications therefore usually manual or semi-automatic standard techniques are used, supplemented by more sophisticated methods – if available.

If multimodal imaging is used, geometric matching of the images is required. The determination of corresponding global or local transformations is the problem of *registration*. Many algorithms have been proposed, see e.g. [10], working on segmented or on non-segmented images. The problem of matching arises also, when medical image data have to be superimposed to an anatomical atlas.

A general problem in medical imaging is that soft-tissues structures are deformable and their shape, size, and orientation may change from the time they are imaged to the time when operative interventions take place. This creates a demand for real time intraoperative imaging, reconstruction and planning methods.

2.3 Examples of Therapy Planning

2.3.1 Surgical Planning

Orthopaedics Surgical planning is used in orthopaedics for many reasons, e.g. to allow the surgeon accomplish accurate preoperative planning and test alternative surgical procedures, to perform a difficult aspect of a surgical procedure, or to select a suited implant based on mechanical simulations. Such a planning can also be very useful if delicate tasks like spinal surgery have

to be performed, where it is important to avoid hurting adjacent structures such as nerves, spinal chord and vessels. The planning requires the execution of geometrical and mechanical simulations for rigid and deformable objects.

Dentistry Computer-aided dental planning, possibly based on computer controlled intraoral radiography, helps to design dental restorations. Computer-assisted manufactoring allows the dentist a fast fabrication of crowns or inlays using numerically controlled micromilling machines. Finite-element caclulations make biomechanical simulations possible to analyze stress and strain in the mandible.

Minimal-Invasive Surgery In endoscopic surgery long thin instruments such as light source, camera, graspers, scissors, lasers, electrocoagulators, and irrigation-aspiration devices are inserted through small incisions or orifices to operate with minimal damage to healthy areas. Often the intervention is visually controlled on a monitor displaying an image taken by a CCD video camera that is located either at the endoscope tip or the surgeons's end of the tube. This surgical technique is becoming more and more prevalent. It comprises interventions of any area of the body, including the gastrointestinal tract, abdomen (laparoscopy), chest (thoracoscopy), or joints (arthroscopy). The obvious advantages are less postoperative pain and faster recovery, resulting in lower costs through shorter hospital stays.

However, there are perception and manipulation problems in endoscopic surgery. These are mainly due to loss or significant reduction of tactile sense and force feedback, dexterity limitations, less degrees of freedom, and restricted visual feedback, especially lack of an overall 3D-view of the operative field.

A solution that offers better guidance to the surgeon is to create an anatomical 3D reconstruction of the surgical space (based on CT, MR or ultrasound images), to supply endoscope instruments with tracking systems, and to display their current position superimposed on the reconstructed 3D scene. Such a system using virtual reality technology can reduce the risk of dangerous movements during surgery. Complementing it with algorithms to simulate movement and functioning of surgical instruments in the 3D scene of continously deformable objects, pre-operative surgical planning and training on realistic models become possible.

Cranifacial Surgery The aim of cranifacial surgery it to reshape human skulls. The reconstructive interventions range from plastic facial surgery carrying out minor cosmetic corrections, to serious operative interventions

giving a skull or face that has been disfigured by a trauma, tumor or other disease, a normal appearance. In facial reconstructive surgery deficient areas are reconstructed with prosthetic materials, or bones are cutted apart and the fragments are repositioned, possibly with the use of bone graft material to fill gaps between bone fragments.

To achieve satisfactory aesthetic results surgery planning is necessary. Cranifacial planning comprises the simulation of the surgery (bone displacement, transplantation and prosthesis) as well as prediction of the 3D soft-tissue deformation based on physical models for facial tissue and skin.

Neurosurgery Neurosurgery requires high geometrical accuracy since severe functional impairment can result if a critical structure is injured due to a minor positioning error. While anatomical landmarks are rare in the brain, it is relatively fixed with respect to the skull. The use of a stereotactic frame to establish an accurate and stable coordinate system for the surgical field has therefore become a common practice.

To define a plan of action surgical planning is necessary: one has to define the target points and volumes and the safest possible approach to the lesion that causes the least possible damage to healthy anatomic structures. The planning has to be based on precise data of different medical imaging modalities that deliver complementary informations and that have to be fused: CT for bone structures, MRI for normal gray and white matter brain anatomy, DSA for vascular anatomy, MEG, high field MRI, and PET for metabolic information. In addition, computer based brain atlases are used.

To utilize the precise quantitative information that imaging databases and surgery planning provide, sophisticated techniques have to be applied during surgery: stereotactic systems, ultrasound and doppler imaging for accurate localization during neurosurgical operations, robotic instruments for precise microsurgery, and several methods such as electroencephalography (EEG) for intraoperative monitoring.

2.3.2 Oncological Treatment Planning

Radiotherapy In radiotherapy beams of photons, electrons, or heavy charged particles (protons or ions) are used to irradiate tumors. The irradiation is limited by the radiation toxicity to healthy tissue, especially if organs at risk are situated in the neighbourhood of the tumor. Radiation treatment is typically performed 20-30 times (fractionation), to give normal tissue a better chance to recover from radiation exposure. To achieve favourable dose distributions usually several directions of incidence are chosen.

Increasing the radiation doses selectively to the tumor can improve cure rates. The general aim therefore is to achieve a geometric shaping of the dose distribution, that conforms to the shape of the tumor and excludes normal tissue from the high dose region (conformal radiotherapy). So-called multi-leaf collimators have been developed, which make it possible to adjust the beam cross-section according to the shape and size of the target volume, as seen from the location of the radiation source for each direction of incidence. Such devices are controlled by a computer-assisted system. In future also intensity modulation of the beam will be possible. Employing such techniques allows the therapist to generate complex spatial dose distributions, e.g. for the treatment of tumors with concave shape enclosing a radiosensitive healthy organ.

Obviously the optimal control of all parameters of such a device is a difficult mathematical problem. But also with less degrees of freedom and simpler radiation devices a detailed treatment plan is required for an optimal treatment of an individual patient. In fact, radiotherapy is the field with longest history in planning.

Treatment planning starts with the definition of therapy-relevant volumes (tumor, radiation sensitive normal tissues) on base of registrated and segmented MRI, CT, or PET images. The conventional procedure, known as forward treatment planning, is as follows: A set of treatment parameters is selected, for example beam directions, beam shape, beam weights, possibly intensity modulation. The corresponding dose distribution within the patient is calculated and evaluated. For this biophysical dose-response relationships should be taken into account. The whole procedure is iterated several times, and the best set of treatment parameters is selected.

The increasing number of treatment parameters available with modern radiation therapy devices makes it unpracticable or even impossible to find an optimal plan by forward planning. Therefore methods are being developed to enable a so-called inverse treatment planning. This means that a desired treatment outcome has to be defined and the treatment parameters resulting in the best approximation to this outcome are determined by an automatic optimization method on a computer.

A state-of-the-art treatment planning system therefore requires a seamless integration of all the following techniques: aquisition of 3D medical images like CT and MRI, 3D registration and segmentation, fast and precise algorithms for 3D dose calculations, fast optimization algorithms, 3D visualization, on-line steering and on-line control of treatments [2].

Hyperthermia Heating tissue cells to temperatures above 41° C affects them. They become sensitized against radiation and cytotoxic pharmaceutica due to the impairment of innercell repair mechanisms and they start to die at temperatures higher than 44° C. This can be exploited to improve the therapeutic efficiency of radiotherapy and chemotherapy by combining these with hyperthermia treatments.

Heat deposited somewhere in the body spreads due to heat transport, mainly by blood circulation. This renders local heating more difficult, but has also some favourable effects. First, combining heating with chemotherapy, cells affected less by pharmaceutical substances due to bad blood supply will become warmer during thermal treatment. Second, some types of cancer tissue are less supplied with blood than healthy tissue. This facilitates the concentration of heat to pathological tissue.

For these reasons hyperthermia, applied in combination with standard oncological therapies, has been recognized as a promising supplementary method in cancer therapy. Basic requirement for a successful application however is an *individual treatment plan* to achieve optimal heating.

How can heat be transported into deep tissue regions and focused to the tumor ? Externally applied infrared radiation can only be used to warm peripheral layers of the human body; due to the good blood supply of these layers the heat deposited there equilibrizes quickly in the body. Ultrasound waves offer a good penetration depth but the waves are strongly reflected on bony structures and therefore are difficult to focus. The standard method to heat deep seated tumors non-invasively is radiation by electromagnetic waves. Usually a wavelength of about 30 cm (i.e. near the microwave domain) is chosen, representing a good compromise between penetration depth and focusability. Several antennas or groups of antennas are used, each of which can be steered independently in wave amplitude and phase, to achieve favourable interference patterns.

To obtain antenna parameters that lead to an optimal temperature distribution, extensive numerical simulations have to be performed in preparation of an individual treatment [38].

2.4 Requirements for Medical Planning Systems

Despite the many application-specific details it seems economical to build a general framework for medical planning. It should provide both basic functionality for all tasks common to medical planning applications as well as adaptability to specific needs of different therapy forms. Abstracting from the huge set of application-specific details and focusing on the common requirements, the required functionality includes components

- to import medical image data of different modalities (preferably conforming to standards like PACS and DICOM)
- to fuse (registrate) possibly distorted image data of different modalities
- to build a patient-specific geometrical model of anatomic or pathologic structures; this includes
  - segmentation of image data, i.e. determination of homogenous regions that constitute a tissue compartment
  - approximative geometrical, possibly multi-resolution representation of tissue boundaries
- to numerically simulate essential phenomena and to optimize treatments (comprising such different fields as simulation of continously deformable anatomical structures, radiation or thermal treatment, cell growth, etc.)
- to monitor physical and physiological quantities during treatment
- to control actuators on-line
- to display in 2D or 3D (possibly using VR technology) and in arbitrary combination data like
  - geometries (polygonal and spline surfaces – representing anatomical structures or medical instruments –, finite-element grids, and other geometrical objects)
  - scalar and vector fields in R, R^2, R^3 and on surfaces.

In summary the main components of such a framework are modules for 3D surface reconstruction, grid generation, numerical simulation, and visualization.

Other general requirements are facilities to modify data interactively in all steps of the planning process, and provision of quantitative visualization methods, for example to query information at arbitrary spatial locations or to generate profiles along arbitrary directions. Probably the most challenging requirement on medical planning software is usability in clinical routine, implying ease of use, robustness, and simplicity.

3 The Medical Planning System HyperPlan

3.1 Software Design

The HyperPlan system developed at ZIB is intended to serve both as an versatile experimental environment for medical research and as a useful tool in clinical practice. Therefore the system is designed to be rather flexible, easily to extend, and customizable. It offers the user an easy-to-use interface with powerful 3D interaction methods, and provides state-of-the-art techniques for graphical and numerical tasks.

Instead of relying on existing visualization and simulation packages, HyperPlan is built as a framework of its own. To limit the expenditure of programming labor and to participate on the rapid development of computer graphics software, a number of powerful object-oriented class libraries are used. In particular, all graphics are implemented on top of OpenGL and the Open Inventor graphics toolkit [31]. The Open Inventor class library facilitates the development of complex 3D applications by providing a hierarchical data structure, in which various geometric objects as well as interactive components, so-called draggers and manipulators, can be represented. The powerful 3D geometry file format defined by Open Inventor makes it easy to transfer geometric models generated by HyperPlan into other packages or into VRML, the standard geometry format used in the world wide web. Furthermore, any kind of external geometry can be easily imported.

Currently HyperPlan runs on SGI platforms only. However, as soon as sufficient 3D graphics performance is avaible on low-cost platforms, the system can be easily ported to PCs, where OpenGL and X Windows are available.

3.2 System Overview

A typical HyperPlan session begins with loading patient specific data, for instance tomographic images or a previously generated finite element grid. Data objects are represented as icons in a *work area*. Each type of data object may be visualized using a number of different methods. These visualization methods are implemented by so-called *display modules*. Each data icon provides a pop-up menu allowing the user to select suitable display modules, which can be 'linked' to the data. In this way a graphical network is constructed, indicating which data is visualized by which module. The resulting three-dimensional scene may be viewed from multiple directions in different windows. Fig. 1 shows an example of the HyperPlan user interface.

Display modules do not necessarily operate in a stand-alone fashion, but there may be dependencies between them. For example there are *overlay*

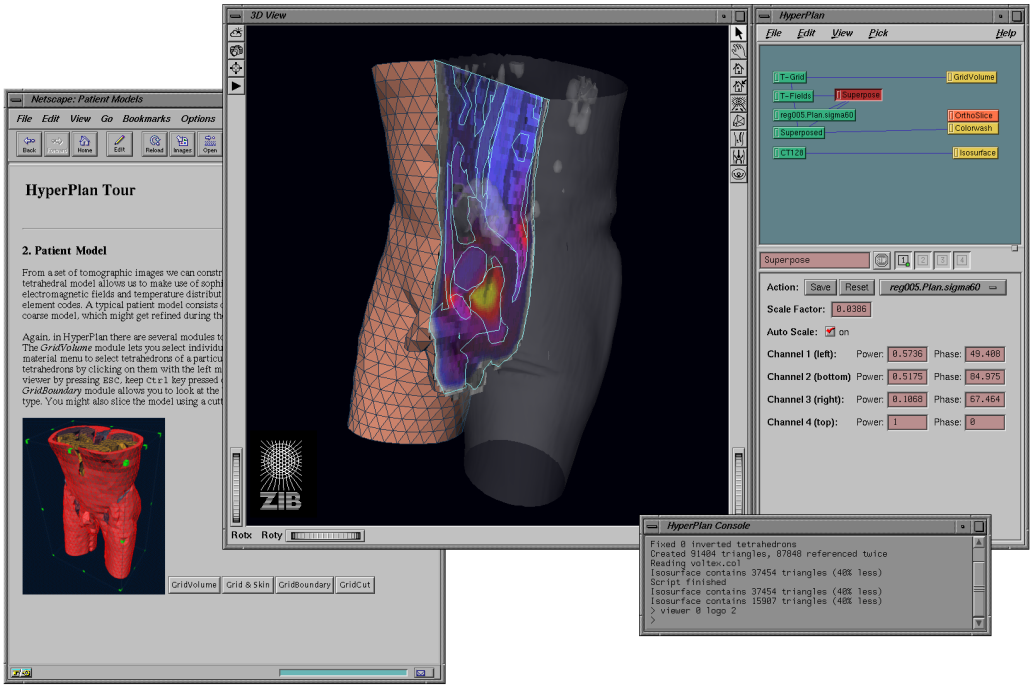

Figure 1: User interface of the HyperPlan treatment planning system consisting of HTML-based help system, 3D viewer, work area, and console window.

modules which require some other module to provide a suitable planar background on which isolines or tissue boundaries can be drawn. These dependencies are also indicated in the work area.

The set of modules can easily be extended without recompiling. This is achieved by means of a resource file, informing the system about what data types can be handled by which module and about further dependencies between modules. Loading and activating modules is delayed until really needed by using a run-time loader. Modules which are not in use do not consume any system resources.

Beside data objects and display modules in HyperPlan there are other components such as *computational modules* or *editors*. Computational modules perform some computation on their input data and put the resulting data objects back into the work area. They are primarily used for tasks which can be performed almost automatically. On the other hand, algorithms which require a significant amount of user interaction, e.g. contouring, are implemented by special-purpose editors. Editors modify their input data directly.

3.3 Segmentation

In HyperPlan manual or semi-automatic standard segmentation techniques are provided. In the following we will outline very briefly some of these methods.

3.3.1 Manual Segmentation

Manual segmentation in 2D means that the user has to define either one-dimensional contours or two-dimensional regions by hand. This task very much resembles the work in a draw or paint system. Contours may be defined point by point as straight line segments or as spline curves. Regions are commonly defined by tagging all corresponding pixels with a pen. A common computer mouse is not very well suited as an input device, although it is still used commonly for manual image segmentation. Better results are obtained with a graphics tablet or with a high resolution digitizer.

3.3.2 Semi-Automatic Algorithms

Manual 2D contouring algorithms can be significantly improved by making the contour an active object instead of a static one. The idea is that a contour loosely defined by the user automatically aligns to edges in its local neighbourhood. There are two different kinds of active contour models, dynamic ones and discrete ones. In dynamic methods or so-called snake algorithms [15, 9] a manually defined contour is interpreted as an elastic ribbon, which deforms under various internal and external forces. The forces are chosen in such a way that the ribbon is attracted by certain edge features in the medical image. On the other hand, in discrete methods integer costs are defined for a contour, which are to be minimized by the contouring algorithm. Again the costs are chosen such that contours following an edge are preferred. A particular powerful variant of a discrete active contour model are so-called *intelligent scissors* [24], which have also been implemented in HyperPlan. This method finds an optimal contour on the fly while the user scetches the coarse shape of the contour [30].

Another simple class of semi-automatic segmentation algorithms are region growing methods. Here the user merely defines a seed point, from which the region growing process is started. Given a criterion which decides if a pixels belongs to the region or not, adjacent pixels are added recursively. As a criterion thresholding, statistical properties, or more advanced textural features can be used. An advantage of region growing methods is, that they can be easily extended to the 3D case.

Currently we are implementing a 3D watershed transformation for multiresolution image segmentation, based on the algorithm given in [36]. This also poses new requirements concerning 3D interaction.

3.4 Grid Generation

In medical planning systems often numerical simulations of physical or physiological processes inside the patient have to be performed. For patient specific treatment planning a geometric *patient model* is needed in which all relevant tissue compartments are represented. In our specific application of hyperthermia planning we are using adaptive multilevel finite element algorithms (see Sect. 3.5.1). To achieve accurate results it is important that the geometric model includes a faithful representation of the interfaces between tissue compartments. Thus we are using *tetrahedral grids* as patient models.

Essentially two steps are needed to generate a tetrahedral grid from the results of segmentation: first a surface model is reconstructed, then the volume between the surfaces is filled with tetrahedra.

3.4.1 Generating a Surfaces Model from 2D Contours

The results of 2D segmentation can be represented by polygonal contour lines describing the boundaries of different tissue compartments. As a first step a coarsening of the contours is performed, i.e. the number of vertices is reduced. This can be done by simply removing inner contour points until the distance or the area between the transformed contour and the initial one exceeds a certain value. A more sophisticated approach uses a discrete wavelet transform [22].

The next step is the *3D reconstruction* of the tissue compartments, i.e. reconstructing the compartments' surfaces from a stack of contours. This is usually done by connecting contours in subsequent slices with triangles.

A fast and fully automatic approach to 3D reconstruction is implemented for example in the *Nuages* package developed at INRIA [11]. Here a 2D Delaunay triangulation is performed for the interior of each contour. Then the triangles in subsequent slices are connected by tetrahedra exploiting the Voronoi diagrams of the 2D triangulations. The outer surface of the resulting tetrahedral grid is used as the compartment surface. Unfortunately this approach cannot handle points where three or more compartments join.

Therefore at present we are using a triangulation algorithm that automatically generates minimal surfaces. The shape of the resulting surfaces can be controlled by interactively prescribing edges between contours. Interactive input is necessary if a branching of a tissue compartment occurs between

subsequent slices. Surface generation for a patient model for hyperthermia planning currently needs 1-2 hours due to the user interaction needed.

3.4.2 Generating a Surface Model from 3D Segmentation

The result of a 3D segmentation can be represented as an assignment of a specific tissue type to each voxel of a 3D medical image. A very simple way to create the compartments' surfaces from this type of information is to search for all pairs of neighbouring voxels with different tissue types, collect the rectangular interfaces between them and construct the surfaces from that interfaces. However, often staggered surfaces result from this approach, especially if the slice distance is large compared to the pixel size.

Smoother surfaces can be obtained using a *marching cubes* algorithm [16] (c.f. Sect. 3.6.1) to extract the compartment interfaces. However, special care must be taken in the vicinity of points or edges connecting three or more compartments.

3.4.3 Generating the Finite Element Grid

To get a volumetric grid the boundary surface of each tissue compartment has to be filled with tetrahedra. We use a 3D *advancing front* algorithm for this purpose. At the beginning the advancing front is identical to the compartment's boundary. Then repeatedly a triangle of the advancing front is selected and a fourth point is searched such that the resulting tetrahedron resembles an equilateral one as much as possible. This procedure is continued until the whole volume is filled with tetrahedra. Our algorithm is derived from the one of Jin and Tanner [13], but uses a faster strategy for selecting the fourth point. To speed up the intersections tests between a given tetrahedon and triangles of the advancing front the triangles are sorted in a tree structure according to their bounding boxes. The complexity of the whole algorithm is $O(N \log N)$, where N is the total number of tetrahedra. The CPU time to generate a complete patient model consisting of more than 30 000 elements is about 5 min on a workstation. An example of a patient model placed in a hyperthermia applicator is shown in Fig. 2.

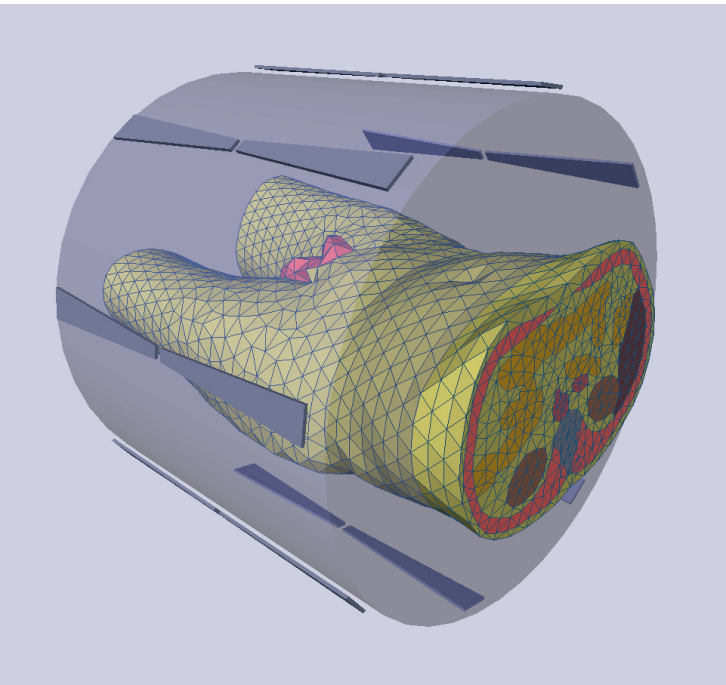

Figure 2: Finite element grid representing the anatomy of a patient and the surrounding antennas of a radiofrequency hyperthermia applicator.

3.5 Numerical Methods

A common requirement concerning numerical simulation is its tight coupling to all other components in the planning system. Users need an integrated environment that provides numerical methods beside 3D reconstruction and visualization components, and that offers a uniform interface to all these components as well.

The numerical techniques to be provided in a medical planning system are more application-specific than that of segmentation, grid generation and visualization. In the following we therefore concentrate on our key application: hyperthermia treatment planning.

The goal of the numerical simulations in this application is to provide a-priori information for the optimal adjustment of wave amplitude and phase of the antennas which generate the fields in radiofrequency hyperthermia. The numerical simulation involves three steps: the calculation of electromagnetic fields and the resulting temperature distribution, as well as an optimization of the temperature distribution according to some quality functional.

3.5.1 Adaptive Finite Element Methods for the Solution of Partial Differential Equations

Many natural phenomena are described by partial differential equations in space and time. In radiofrequency hyperthermia the governing physical laws are Maxwell's equations modelling the electromagnetic fields radiated by the antennas, and a heat transfer equation, modelling the essential transport mechanisms in human tissue.

We are employing finite element methods for the numerical solution of these partial differential equations. In both cases we use a tetrahedral mesh for the discretization of the solution area to get a faithful representation of complicated tissue boundaries. Our finite element algorithms are based on adaptive mesh refinement [7], i.e. the finite element grid is improved in regions where the numerical solution does not have the required precision. These adaptive techniques are driven by error estimators, which yield an estimate of the local discretization error in the calculated field.

We consider these procedures of crucial importance, as the user of a planning system usually does not have sufficient information to construct problem-specific discretizations or to check the reliability of a numerical solution.

Maxwell's Equations As the antennas of our applicator are driven with a fixed angular frequency ω, we can neglect initial transients in the fields and are left to solve Maxwell's equations in the frequency domain:

$$\begin{aligned} \nabla \times \mathbf{H} &= \mathbf{j} + i\,\omega\,\mathbf{D} & \qquad \nabla \cdot \mathbf{B} &= \mathbf{0} \\ \nabla \times \mathbf{E} &= -i\,\omega\,\mathbf{B} & \qquad \nabla \cdot \mathbf{D} &= \rho \end{aligned}$$

The fields $\mathbf{E}, \mathbf{H}$ and the flux densities $\mathbf{D}, \mathbf{B}$ are related by the material equations $\mathbf{D} = \epsilon\,\mathbf{E}$ and $\mathbf{B} = \mu\,\mathbf{H}$, where ϵ represents the dielectric 'constant' and μ denotes the permeability. The current density $\mathbf{j}$ can be obtained from Ohm's law $\mathbf{j} = \sigma\,\mathbf{E}$. As the fields have been introduced as complex variables, $\mathbf{j}$ can be accounted for by defining a complex dielectric constant ϵ_c:

$$\begin{aligned} \nabla \times \mathbf{H} &= \sigma\,\mathbf{E} + i\,\omega\,\epsilon\mathbf{E} \\ &= i\,\omega\,(\epsilon - i\sigma/\omega)\mathbf{E} \;=\; i\,\omega\epsilon_c\mathbf{E}\,. \end{aligned}$$

For the finite element method, we use a variational principle based on the double-curl equation, where an electrical field $\mathbf{E}$ is sought which causes the functional

$$F(\mathbf{E}) \;=\; \frac{1}{2}\int \left\{ \frac{1}{\mu}(\nabla \times \mathbf{E})(\nabla \times \mathbf{E}^*) \;-\; \omega^2\epsilon\,\mathbf{E}\mathbf{E}^* \right\} dV$$

to be stationary.

In dielectric media no free charges and surface currents are present. Then a standard consideration shows that on interfaces between different media 1 and 2 the continuity relations for the electromagnetic field components are

$$\begin{aligned} \mathbf{n} \times (\mathbf{E_2} - \mathbf{E_1}) = 0 \qquad &\Rightarrow \quad E_2^{\parallel} = E_1^{\parallel} \\ \mathbf{n} \cdot (\mathbf{D_2} - \mathbf{D_1}) = 0 \qquad &\Rightarrow \quad D_2^{\perp} = D_1^{\perp} \quad \Rightarrow \quad \epsilon_2 E_2^{\perp} = \epsilon_1 E_1^{\perp}. \end{aligned}$$

Since tissue interfaces can influence the electromagnetic field considerably, the finite element grid should resolve these boundary contours well. Additionally, care has to be taken to enforce the physical continuity relations of the fields correctly in numerical calculations [26]. The first requirement is fulfilled by using tetrahedral grids, the second one by employing edge elements, sometimes also called Whitney elements [4]. In conjunction with the variational principle above, such basis functions enforce the required continuity of the field.

A specific difficulty arises in the solution of the resulting linear equation systems. Their matrices are indefinite and comprise several tens or even hundreds of thousands degrees of freedoms. We are using multilevel techniques which exploit the hierarchy of finite element grids generated in the adaptive refinement sequence.

An error estimator indicates the regions where the numerical solution does not have the required precision. It is based on a stress-projection method, where the dual magnetic field $\mathbf{H}$ is obtained from the 'working variable' $\mathbf{E}$ by taking a simple derivative due to Maxwell's laws. Then it is improved by an L_2-projection into the original Whitney basis of $\mathbf{E}$. Here an important aspect is the superconvergence property of specific quadrature points in a finite element mesh, allowing such a stress recovery technique. A local comparison gives the desired error estimates.

The 'infinite' space sourrounding the complete arrangement of patient and antenna array is modelled approximately by absorbing boundary conditions [14]. A 3D representation of the electric field inside the patient is displayed in Fig. 3.

The Heat Transfer Equation Due to Ohm's law, the current density $\mathbf{j}$ induced by the electric field $\mathbf{E}$ is $\mathbf{j}(\mathbf{x}) = \sigma(\mathbf{x})\,\mathbf{E}(\mathbf{x})$ in a material with electric conductivity σ. The average power Q deposited by the electromagnetic waves therefore is given by

$$Q(x) = \frac{1}{2}\,\sigma(x)\,\mathbf{E}(x)\mathbf{E}^*(x)\ .$$

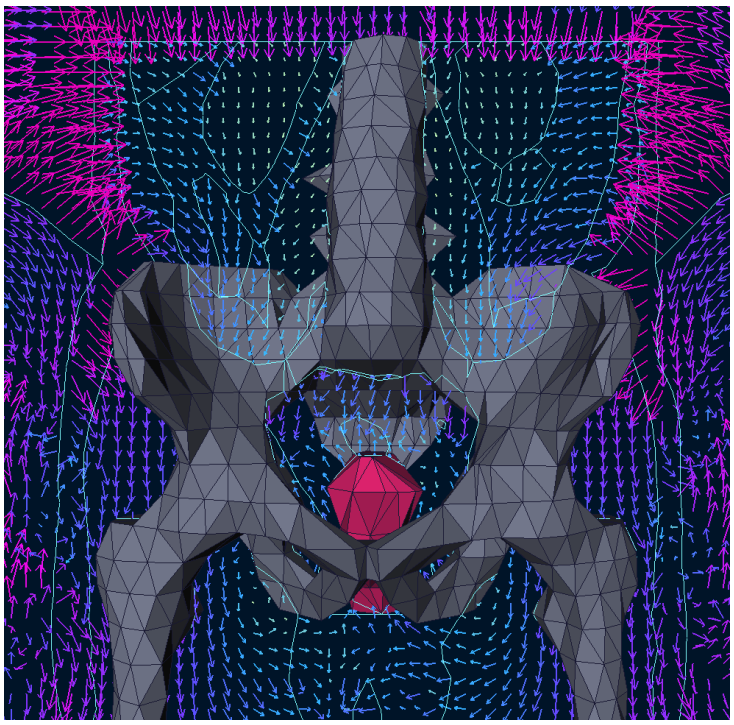

Figure 3: Electric field inside the patient (shown are pelvic bones and the tumor in the pelvis).

If an array of antennas is used, the total field can be computed by a linear superposition of their fields. Representing amplitudes and phases of the feeding voltages by complex amplitudes Z_i for each of the n independent antennas, the absorbed power is a hermitean form of the n amplitudes Z_i.

It is a rather difficult task to model the heat transport in the human body. The main problem is to establish an approximate physical model with parameters known in advance or being obtainable by non-invasive measurements. The most widely used approximate description of heat transport is given by Pennes's bio-heat-transfer equation [25]

$$\rho_t \, c_t \, \frac{\partial T}{\partial t} = \nabla(k \nabla T) \; - \; \rho_b \, c_b \, \rho_t \, W \, (T - T_b) + Q.$$

Here W is an empirical coefficient, strongly related but not equal to the arterial perfusion based on mass flow rates [27]. The equation approximately describes the transient behaviour of the temperature in the tissue. We solve it adaptively both in space and time [5, 3], employing the so-called Rothe method, where time is discretized first. For each time step the finite element mesh is refined due to the momentary temperature distribution. Both time

and space errors are estimated by a defect correction scheme of higher order; they have to be matched appropriately in choosing the step width in time and element size in space. The elliptic linear subsystems arising in the space discretizations of each time step are solved by a multigrid procedure, which provides an optimal computational complexity.

3.5.2 Optimization

The stationary solution ($\partial T/\partial t = 0$) of the bio-heat-transfer equation serves as input for an optimization procedure, which provides optimal values for the amplitudes and phases of the antennas. Writing the temperature as a sum of basal temperature (i.e. $Q \equiv 0$) and temperature increase ΔT (due to non-zero Q), ΔT depends *linearly* on the power distribution Q, which is a hermitean form of the complex amplitudes Z_i. The heating ΔT therefore is also a hermitean form. The hermitean matrices can be derived for all nodes of the finite element grid by calculating the temperature distributions for n^2 independent combinations of complex amplitudes. Hence the stationary temperature distribution can be established very quickly for an arbitrary choice of field amplitudes. In the same way also derivatives of the temperature with respect to the amplitudes can be calculated, rendering fast optimization possible.

A reasonable objective function is one that penalizes temperatures in the tumor below 43° C and temperatures in healthy tissue above 42° C. Similar objective functions are used in radiotherapy, to optimize angle, shape and intensity of the rays. We are employing a damped Newton procedure to solve the optimization problem. The optimization for an applicator with 4 groups of antennas based on a temperature calculation e.g. on a coarse grid of 8 400 nodes or a refined one of 32 100 nodes needs 11 or 40 seconds respectively on a Sun SPARC20. An optimized temperature distribution using 4 groups of antennas is shown in Fig. 6 (p. 25).

3.6 Visualization Methods

In medical treatment planning many data entities of different types are encountered. The data sets are usually quite large. Nevertheless, fast and accurate visualizations methods are needed for successful treatment planning. Often it is important to visualize different data in combination. This allows the user for example to judge how good a reconstructed geometry approximates the real anatomic situation, how numerically calculated quantities depend on the underlying patient model, or which tissue compartments are primarily affected by certain effects.

In recent years several visualization methods have been developed that exploit special hardware features of modern graphics workstations. The most outstanding hardware capabilites are very fast rendering of polygons and support for texture mapping. In contrast to visualization methods implemented in software, e.g. direct volume rendering via ray casting, polygon-based rendering methods exhibit much higher performance. The combination of multiple visualization techniques becomes also easier with these methods. For these reasons we prefer to apply polygon- and texture-based methods.

In the following sections we will outline some of the visualization methods provided in the HyperPlan software system. Mainly these are techniques for displaying scalar fields, also in combination with polygonally defined surfaces. Algorithms for the visualization of vector fields, a task of less general interest in the medical application domain, are described elsewhere [29, 1]. On a fast graphics workstation the presented techniques provide truely interactive performance, i.e. sub-second frame rates. As already mentioned, the algorithms are implemented within the framework of Open Inventor using the OpenGL graphics library.

Externally defined objects can be easily integrated into the system using the Open Inventor 3D geometry file format. Displaying geometric objects like surgical instruments or radiation devices is often quite helpful for the physician. It enables him or her to recognize and adjust the position of the treatment units relative to the patient.

3.6.1 Isosurface Generation using Marching Cubes

The visual representation of scalar volume data (e.g. tomographic images) plays an important role in medical planning. It can be achieved either by generating and displaying a polygonal representation of iso-surfaces, or by direct volume rendering. Direct volume rendering, displaying semi-transparent cloudy structures, yields more comprehensive images. These may include surface-like objects, too. However, volume rendering is computationally very expensive, especially if a gradient dependent shading term is included, and it is fraught with the problem of choosing suitable transfer functions which map data values to color and opacity.

Therefore iso-surfaces still play an important role in medical applications and in scientific visualization in general. Perhaps the most well-known algorithm for generation of iso-surfaces is the marching cubes algorithm [16]. It computes a polygonal approximation of an iso-surface of a scalar field defined on a cartesian grid. This algorithm is the ancestor of many related ones being used in a broad variety of applications today. In medical imaging marching cubes can be used for example to extract bone structures, muscles, or the

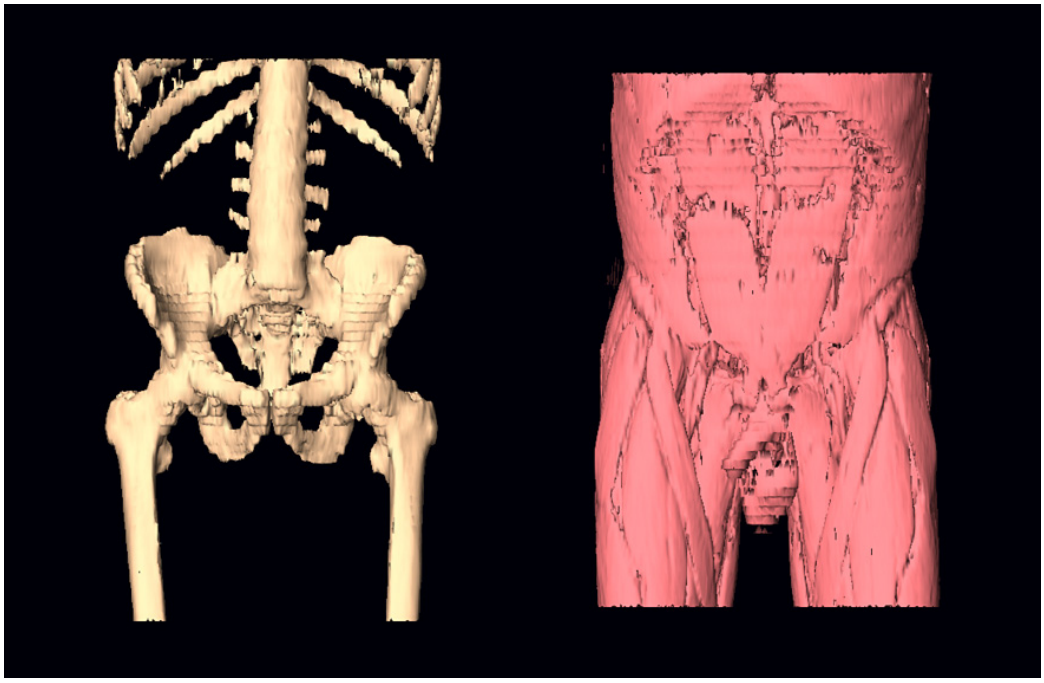

Figure 4: Results obtained by applying the marching cubes algorithm to raw CT data using different thresholds corresponding to bone (left) and muscle (right).

skin surface from CT images. Example images obtained by this method are shown in Fig. 4.

In marching cubes all cells of a cartesian grid are processed separately. The data values are assumed to be defined at the corners of a cell. Given an isosurface threshold, each corner's value may lie below or above. The 256 possible combinations can be reduced to 14 distinct base cases , by considering the symmetries of a cube. For each cell containing a part of an iso-surface the shape of its triangular approximation is read from a lookup table. The vertices of the triangulation are determined by a linear interpolation of the field along the edges of a cell. While the original algorithm possibly produced topological errors, i.e. leaks in the iso-surface, a consistent triangulation can be obtained e.g. by a modified lookup table [17, 20].

For large data sets, such as highly resolved medical image data, standard isosurface algorithms yield a huge number of polygons, often prohibiting real-time rendering even on fast graphics computers. Applying standard polygon reduction algorithms to the results of marching cubes is a practicable but not ideal solution since the information about the underlying scalar field can not enter any more. Instead polygon reduction should happen right during

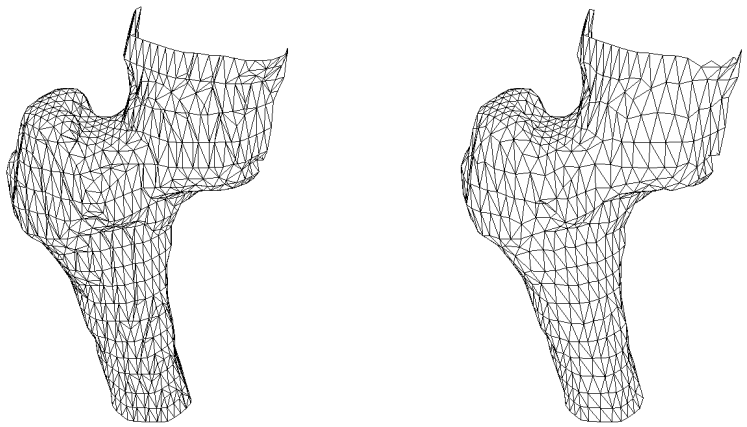

Figure 5: Comparison of isosurfaces generated by the traditional marching cubes algorithm (left) and the compact cubes algorithm (right). The compact cubes algorithm reduces the number of triangles in an isocontour to about 50 percent.

the isosurface calculation. This is accomplished for example by the compact cubes algorithm [21], which reduces the number of polygons to about 40–50% and avoids degenerated triangles. The slight increase in computing time is more than compensated by decreased rendering time. By coalescing certain vertices of an interim surface triangulation into a new single vertex, small triangles of the triangulation are shrinked to a single point. Likewise narrow triangles that emerge when two vertices are close to the same grid point, are collapsed into an edge of the new triangulation. The new polygonal approximation, containing less and much better shaped triangles, differs only slightly from the old contour, see Fig. 5.

3.6.2 Direct Volume Rendering via 3D-Textures

Direct Volume rendering [8] is a powerful, though computationally expensive rendering technique for visualizing 3D scalar fields. The volume of interest is assumed to be filled with a fictitious medium affecting light transport. The scalar data to be visualized is mapped by so-called transfer functions to optical parameters of this medium, like absorption, emission, and scattering coefficients. Then based on a physically motivated transport equation, the resulting radiation field is calculated in the image plane [12]. For performance reasons often simple emission-absorption models are considered. In these models no scattering terms appear. Traditionally the ray-integration

necessary to calculate pixel intensities has been performed by ray-casting (iteration in image space) [19] or by cell projection (iteration in object space) [33]. Recently an alternative method has become popular, which exploits the 3D texture mapping capabilities of modern graphics computers [6, 34]. The method achieves impressing rendering performance for uniform data sets. However, there are some limitations. For example, gradient-dependent illumination models can not be applied currently. This is disadavantageous, since surface like illumination terms are known to provide visual cues that significantly improve spatial perception [19].

To generate volume rendered images of a tomographic image stack, first a transfer function is applied to the original data to obtain some color intensity C and opacity α for each voxel. Usually it is necessary to incorporate segmentation information into this mapping to visually enhance relevant parts of the data volume. Color and opacity values define a three-dimensional texture, which can be loaded directly into the graphics subsystem. This texture is applied to a number of parallel polygons, which are oriented perpendicular to the camera's view direction and which enclose the whole texture cube for all view directions. The volume rendering integral is approximated by drawing and compositing the individual polygons from back to front into the frame buffer. To prevent rendering of the polygons' outer parts, six user defined clipping planes are defined. Typically several hundred slices are taken through the volume. More slices improve image quality at the expense of rendering speed. On hardware platforms with unsufficient texture memory the data has to be split into parts. This makes it necessary to reload the whole 3D texture multiple times during the rendering process.

The method can easily be modified to compute maximum intensity projections (MIP). These are often preferred in medical applications since they make a more quantitative data analysis possible. Another advantage of the 3D texture mapping approach is, that it can be easily combined with the display of lines or surfaces.

3.6.3 Cell Projection for Tetrahedral Grids

While 3D texture mapping is a powerful method for volume rendering of scalar fields defined on a uniform cartesian grid, it cannot be applied to data defined on unstructured grids without resampling the whole data volume. Of course, resampling introduces errors and should therefore be avoided. Direct volume rendering on unstructured grids can be achieved by separately projecting each grid cell into the image plane. The projected geometry of a single cell may be approximated by semi-transparent polygons. In this way modern graphics hardware can be used efficiently. A very simple form

of cell projection algorithms are so-called splatting methods [37, 18]. In these algorithms the projection of an individual cell is approximated by a simple footprint or splat, which looks the same irrespectively of the actual viewing direction. The footprints usually are chosen to be somewhat larger than the cell diameters, causing the data to appear artificially smooth in the final images. This may look nice, but of course is dangerous in medical applications where more quantitative pictures are required.

Instead of using simple splats, therefore the exact cell projection should be computed. This turns out to be quite simple for tetrahedral grids. The projection of a tetrahedron on a plane can be decomposed into three or four triangles, which are arranged around a center point. At this point the projected tetrahedron has its maximal thickness. Shirley and Tuchman [28] suggested to compute color and opacity only for this point as well as for the other vertices of the projection, and then use Gouraud shading to render the individual triangles. Gouraud shading means that color and opacity are interpolated linearly within a triangle, an operation performed by the graphics hardware. This method is exact only if there is constant light emission and light absorption within the whole tetrahedron. An exact solution for linearly varying but proportional emission and absorption can be obtained by rendering texture mapped triangles. Two texture coordinates are used. These are interpreted as depth and emission-absorption coefficients respectively. Again graphics hardware interpolates both parameters linearly within a triangle. The correct color and opacity then is read from a 2D texture map. Like in all cell projection methods some care has to be taken to traverse all tetrahedrons in back-to-front order. This is necessary to ensure a correct compositing of the individual projections. The situation is very much simplified if all triangles have the same color. In this case the final image does not depend on the depth ordering.

In HyperPlan this method is used to visualize 3D scalar fields defined on a tetrahedral grid. Again, it is important that other objects like bone structures or isosurfaces can be combined with this type of volume rendering. This is illustrated in Fig. 6.

4 Conclusions

3D medical imaging methods deliver anatomical and physiological data of the patient's interior. This has changed medical diagnosis. The additional availability of reliable physiological and physical models, efficient numerical algorithms, and powerful affordable computer hardware will also change medical therapy. The possibility of planning a therapy individually by sim-

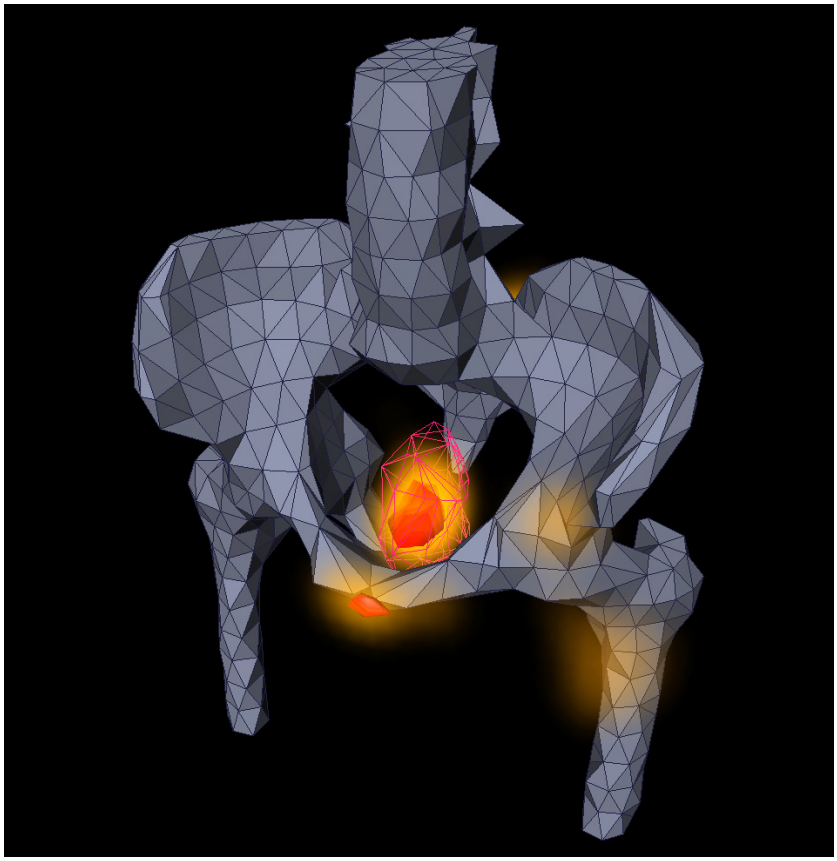

Figure 6: Optimized temperature distribution using eight antennas (volume rendering via cell projection).

ulating suitable mathematical models leads to the emergence of a new field: *quantitative medicine*. To support this new direction, appropriate physical models have to be built, that get along with input parameters obtainable by measurements. Furthermore highly efficent numerical methods and visualization techniques are needed that enable such simulations in a short amount of time. Since in medical treatment planning several complex and tightly linked steps are to be completed, appropriate tools have to be provided within a single software environment.

We presented a platform for medical treatment planning that is intended to serve both as a versatile experimental environment for research and as a beneficial tool in clinical practice. The requirement of utmost importance in the long run will be usability in clinical routine. This will probably lead to highly specialized planning systems that are indivually customized for certain medical applications. However, currently there is a big need for systems ful-

filling both requirements mentioned above. Our planning system HyperPlan has originally been developed for application in regional hyperthermia. However, by abstracting from specific requirements and using general concepts, a rather versatile environment has emerged that can be easily adapted to other medical planning tasks, too. The system embodies efficient algorithms for numerical simulation, as well as powerful techniques for interactive visualization and 3D interaction.

From researchers' point of view the system serves as a tool that allows to explore new methods from algorithmic mathematics, visualization, and medicine in therapy planning. We hope that from the patients' view it will appear as an instrument that helps to improve the efficacy of therapeutical procedures and to minimize the often unpleasant secondary effects of medical treatments.

Acknowledgements

The hyperthermia project is financially supported by DFG (Sonderforschungsbereich 273, "Hyperthermie: Methodik und Klinik"). To Peter Wust, the spiritus rector of the hyperthermia project, we are indepted for valuable discussions on all clinical issues and numerous technical aspects of hyperthermia therapy. For discussions on the electro-technical questions and the provision of a finite-difference Maxwell-solver we are grateful to Jacek Nadobny. Furthermore, we thank Susan Wegner, Helmut Oswald, and Jürgen Beier who helped us to understand segmentation issues and provided segmentation algorithms. For beneficial discussions concerning the design of HyperPlan, contribution of various ideas, and help during implementation, we thank Thomas Anders, Henrik Battke, Tobias Höllerer, Roland Wunderling, and Malte Zöckler.

References

[1] H. Battke, D. Stalling, H.-C. Hege, *Fast Line Integral Convolution for Arbitrary Surfaces in 3D*, in: H.C. Hege, K. Polthier (eds), Visualization and Mathematics, Springer, 1997, to appear.

[2] R. Bendl, J. Pross, M. Keller, J. Bürkelbach, and W. Schlegel, *VIRTUOS - A program for VIRTUal radiOtherapy Simulation*, in: H.U. Lemke et al. (eds), Computer Assisted Radiology, Berlin, Springer, (1993) 676–682.

[3] F. Bornemann, *An Adaptive Multilevel Approach to Parabolic Equations, part III: 2D-error estimation and multilevel preconditioning*, IMPACT Comput. Sci. Engrg. 4 (1992), 1–45.

[4] A. Bossavit, *Whitney forms: a class of finite elements for three-dimensional computation in electromagnetism*, Inst. Elec. Eng. Proc., Part A, 135:8 (1988), 493–500.

[5] F. Bornemann, B. Erdmann, R. Kornhuber, *Adaptive multilevel-methods in three space dimensions*, Int. J. Numer. Meth. Eng. 36 (1993), 3187–3203.

[6] B. Cabral, N. Cam, J. Foran, *Accelerated Volume Rendering and Tomographic Reconstruction Using Texture Mapping Hardware*, in: Proceedings of the Symposium on Volume Visualization, 1994, 91–98.

[7] P. Deuflhard, P. Leinen, H. Yserentant, *Concepts for an adaptive hierarchical finite element code*, IMPACT Comput. Sci. Engrg. 1 (1989), 3–35.

[8] R.A. Drebin, L. Carpenter, P. Hanrahan, *Volume Rendering*, Computer Graphics 22:4 (1988), 65–74.

[9] R. Ďurikovič, K. Kaneda, H. Yamashita, *Dynamic contour: A texture approach and contour operations,* The Visual Comp. 11 (1995), 277–289.

[10] P. A. Van den Elsen, E. Pol, M.A. Viergever, *Medical image matching – A review with classification*, IEEE Engineering in Medicine and Biology, 12:1 (1993), 26–39.

[11] B. Geiger, *Three-dimensional modeling of human organs and its application to diagnosis and surgical planning*, Technical Report 2105, Institut National de Recherche en Informatique et Automatique, (France), Dec 1993.

[12] H.C. Hege, T. Höllerer, D. Stalling, *Volume Rendering: Mathematical Models and Algorithmic Aspects,* ZIB Techn. Rep. TR 93-7 (May 1994), 36 p.

[13] H. Jin, R. Tanner, *Generation of three-dimensional unstructured grids by the advancing front technique*, Int. J. Num. Meth. Eng. 36 (1993), 1805–1823.

[14] V.N. Kannelopoulos, J.P. Webb, *Numerical study of vector absorbing boundary conditions for the finite element solution of Maxwell's equations,* IEEE Microwave Guided Wave Lett., 1 (1991), 325–327.

[15] M. Kass, A. Witkin, D. Terzopoulos, *Snakes: active contour models,* Int. J. Comput. Vis. 4 (1987), 321–331.

[16] W.E. Lorensen, H.E. Cline, *Marching cubes: A high resolution 3D surface construction algorithm*, Computer Graphics 21:4 (1987), 163–169.

[17] W.E. Lorensen, *Extracting Surfaces from Medical Volumes*, in: Visualization '94, Course Notes: Volume 13, *Visualization Algorithms and Applications* (1994), 26–45.

[18] D. Laur, P. Hanrahan, *Hierachical Splatting: A Progressive Refinement Algorithm for Volume Rendering*, Computer Graphics (SIGGRAPH '91 Proceedings) 25:4 (1991), 285–288.

[19] M. Levoy, *Display of Surfaces from Volume Data*, IEEE Computer Graphics and Applications 8:3 (1988), 29–37.

[20] C. Montani, R. Scateni, R. Scopigno, *A modified look-up table for implicit disambiguation of marching cubes,* The Visual Comp., 10:6 (1994), 353-355.

[21] D. Moore, J. Warren, *Mesh Displacement: An Improved Contouring Method for Trivariate Data*, Technical Report TR-91-166, Rice University, Department of Computer Science, 1991.

[22] D. Meyer, *Multiresolution Tiling*, Proceedings of Graphics Interface '94, Canadian Information Processing Society, May 1994, Banff, Alberta (Canada) 1994, 25–32.

[23] J.-M. Morel, S. Solimini, *Variational Methods in Image Segmentation,* Progress in Nonlinear Differential Equations and Their Applications, Vol. 14, Birkhäuser, Boston, 1995.

[24] E.N. Mortensen, W.A. Barrett, *Intelligent Scissors for Image Composition,* in: R. Cook (ed.), SIGGRAPH 95 Conference Proceedings, Annual Conference Series, 1995, 191–198.

[25] H. H. Pennes, *Analysis of tissue and arterial blood temperatures in the resting human forearm*, Journal of Applied Physiology 1 (1948), 93–122.

[26] K.D. Paulsen, X. Jia, J.M. Sullivan, *Finite element computations of specific absorption rates in anatomically conforming full-body models for hyperthermia treatment analysis*, IEEE Trans. Biomed. Engrg., 40:9 (1993), 933–945.

[27] R. B. Roemer, A. W. Dutton, *A new tissue convective energy balance equation for predicting tissue temperature distributions*, presented at: ICHO VII, Rome, Italy, April 9-13, 1996; Univ. at Utah preprint 1996, Mechan. Eng. Dept. and Radiation Oncology Dept., Salt Lake City, Utah.

[28] P. Shirley, A. Tuchman, *A Polygonal Approximation to Direct Scalar Volume Rendering*, Computer Graphics 24:5 (1990), 63–70.

[29] D. Stalling, H.C. Hege, *Fast and Resolution Independent Line Integral Convolution,*, Proceedings of SIGGRAPH '95, (Los Angeles, California, August 6-11,1995). In *Computer Graphics* Annual Conference Series, 1995, 249–256.

[30] D. Stalling, H.-C. Hege, *Intelligent Scissors for Medical Image Segmentation,* in: B. Arnolds, H. Müller, D. Saupe, T. Tolxdorff (eds), Tagungsband zum 4. Freiburger Workshop "Digitale Bildverarbeitung in der Medizin", Freiburg, 14.-15. März, 1996, 32–36.

[31] P.S. Strauss, R. Carey, *An object-oriented 3D graphics toolkit*, Computer Graphics (SIGGRAPH '92 Proceedings) 26:4 (1992), 341–349.

[32] J.K. Udupa, R.J. Gonçalves, *Imaging Transforms for Volume Visualization,* in: R. H. Taylor, S. Lavallée, G.C. Burdea, Ralph Mösges (eds.), Computer-Integrated Surgery, MIT-Press, Cambridge MA, 1996.

[33] C. Upson, M. Keeler, *V-Buffer: Visible Volume Rendering*, Computer Graphics 22:4 (1988), 59–64.

[34] O. Wilson, A. Van Gelder, J. Wilhelms, *Direct Volume Rendering via 3D-Textures*, Technical Report UCSC-CRL-94-19, University of California, Santa Cruz, 1994.

[35] S. Webb, *The Physics of Medical Imaging,* (Medical Science Series) Bristol, UK, 1988, IOP Publishing.

[36] S. Wegner, T. Harms, H. Oswald, E. Fleck, *The Watershed Transformation on Graphs for the Segmentation of CT Images*, Proc. of 13th International Conference on Pattern Recognition, Vienna 96, 1996, 498–502.

[37] L. Westover, *Footprint Evaluation for Volume Rendering*, Computer Graphics 24:4 (1990), 367–376.

[38] P. Wust, J. Nadobny, R. Felix, P. Deuflhard, A. Louis, W. John, *Strategies for optimized application of annular-phased-array systems in clinical hyperthermia*, Int. J. Hyperthermia 7 (1991), 157–173.